Soft Matter

RSC Publishing

PAPER

View Article Online
View Journal | View Issue

The 'Sticky Elastica': delamination blisters beyond small deformations†

Cite this: *Soft Matter*, 2013, **9**, 1025

Till J. W. Wagner[a] and Dominic Vella*[b]

We consider the form of an elastic loop adhered to a rigid substrate: the 'Sticky Elastica'. In contrast to previous studies of the shape of delamination 'blisters', the theory developed accounts for deflections with large slope (*i.e.* geometrically nonlinear). Starting from the classical Euler Elastica we provide numerical results for the dimensions of such blisters for a variety of end–end confinements and develop asymptotic expressions that reproduce these results well, even up to the point of self-contact. Interestingly, we find that the width of such blisters does not grow monotonically with increased confinement. Our theoretical predictions are confirmed by simple desktop experiments and suggest a new method for the measurement of the *elastocapillary length* for deformations that cannot be considered small. We discuss the implications of our results for applications such as flexible electronics.

Received 17th August 2012
Accepted 8th November 2012

DOI: 10.1039/c2sm26916c

www.rsc.org/softmatter

1 Introduction

Delamination blisters are often the undesired consequence of an adhesive film placed imperfectly on a substrate. They are the nemesis of anyone trying to wrap Christmas presents using sticky tape and regularly frustrate smartphone users who want to put a protective film on their phone screen. Blisters appear when an adhered film is subject to an in-plane compressive strain relative to the substrate. Such a strain can result from a differential compression (*e.g.* due to heating) or because of a mismatch between substrate and film geometries.[1–4] Even small mismatches can give rise to significant blisters, which can, in turn, greatly affect the functionality of the adhering film in applications from protective coatings to the conduction characteristics of few layer graphene sheets.[5–7]

Historically, delamination blisters have found use as a simple means of measuring the strength of adhesion between two materials, a series of methods known as *blister tests*.[8–12] However, more recently, and in spite of some of the negative connotations of delamination, it has been proposed that partial delamination and buckling of thin adhesive sheets can be intentionally integrated into the design of flexible electronic devices.[13–16] In these devices, the conducting components are only adhered to the substrate in some regions and not others; this 'blistered' shape allows them to accommodate the flexure of the substrate without deforming plastically. In current flexible electronic applications the form of these blisters is controlled by patterning the substrate with a periodic variation in adhesive strength. However, such techniques may suffer from the spontaneous formation of delamination blisters with a well-defined size;[3,17] understanding the size and form of such blisters is important since their characteristic curvature can damage the conducting components.[13,18]

While the formation of delamination blisters is a classical problem, previous analyses have focussed on the limit of blisters with a small slope (small deformations). However, in many new applications, this restriction is inappropriate. The shape of a highly deformed elastic strip, commonly referred to as an 'Elastica', has been widely studied since the time of the Bernoullis and Euler.[19] Indeed, research continues on the contact of an Elastica with a rigid boundary.[20,21] However, the combination of adhesion and large deflection elasticity seems only to have been considered for the case of self-contacting 'rackets'.[22,23] In this article, therefore, we consider the form of a blister without the restriction of small slopes — the 'Sticky Elastica'. Using a combination of numerical, asymptotic and experimental techniques we show how the results of previous small deformation analyses may be altered to take into account these large deformations and suggest how experimental data might best be analysed in the light of our results.

2 Theory

We consider an inextensible elastic sheet, resting on a semi-infinite, rigid substrate. The sheet is subjected to an in-plane compression Δl which results in a delamination blister of height d and width ℓ (Fig. 1). The rate of compression is assumed small so that the sheet is in static equilibrium at all times. The shape of the blister is defined by the intrinsic angle $\theta(s)$, (s being the arc-length) and a point on the blister has

[a]*Department of Applied Mathematics and Theoretical Physics, University of Cambridge, Wilberforce Rd, Cambridge, CB3 0WA, UK*

[b]*OCCAM, Mathematical Institute, 24-29 St Giles', Oxford, OX1 3LB, UK. E-mail: dominic.vella@maths.ox.ac.uk*

† Electronic supplementary information (ESI) available. See DOI: 10.1039/c2sm26916c

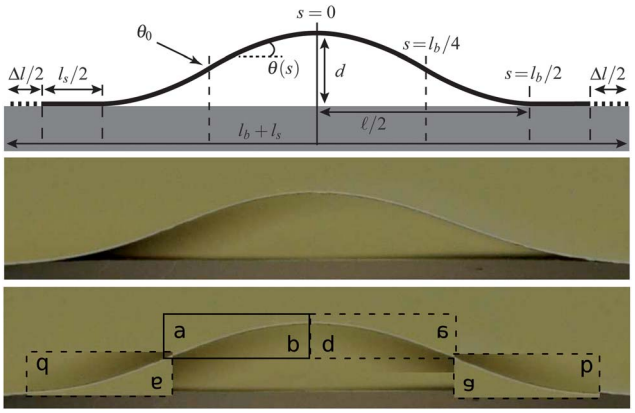

Fig. 1 Top: schematic of a thin sheet resting on an adhesive substrate and subject to an end–end compression Δl. The result is a blister with arc-length l_b and dimensions d and ℓ. Centre: experimental blister ($\ell_{ec} \approx 0.76$ cm), with $\Delta l = 0.03$ cm ($\Delta L \approx 0.04$), leading to $d = 0.17$ cm, $\ell = 1.16$ cm, ($\delta \approx 0.22$, $\lambda \approx 1.53$). Bottom: illustration of the four-fold symmetry of the Elastica; the image in the central panel is reconstructed by taking the segment $-l/4 < s < 0$, (solid frame) and rotating and reflecting to form the other images — inversions of a, b illustrate the different reflexions. Here the sheet thickness $h = 42$ μm.

coordinates $[x(s), w(s)]$ where $dx/ds = \cos\theta$ and $dw/ds = \sin\theta$ arise from geometric considerations. The delaminated portion has arc-length l_b, which is initially unknown. The end-points of the delaminated regions are then given by $s = \pm l_b/2$ and the system is assumed to be symmetric around $s = 0$. Since the sheet remains smooth, we must have that $\theta(\pm l_b/2) = \theta(0) = 0$.

We shall use a variational approach to derive the appropriate governing equation and boundary conditions. In this formulation of the problem, we consider the energy of the system to be composed of a contribution from the bending energy of the sheet and another term from the sheet–substrate adhesion energy, $\Delta\gamma$. (We neglect the effect of the weight of the delaminated portion of the sheet for simplicity. From the heavy elastica equation[24] we see that this assumption is valid provided that $l_b\rho g h/\Delta\gamma \ll 1$, in which ρ is the sheet density, h its thickness and g the acceleration due to gravity.†) We must minimize this combined energy subject to the constraint of an imposed end–end displacement Δl. Supplementing the energy (measured relative to the flat, fully adhered state) with a Lagrange multiplier to enforce this constraint, the problem reduces to the minimization of

$$U = \int_{-l_b/2}^{l_b/2} \left(\frac{1}{2} B\theta_s^{\,2} + \Delta\gamma\right) ds - \alpha\left[l - \Delta l - \int_{-l_b/2}^{l_b/2} \cos\theta ds\right]. \quad (1)$$

Here the first term represents the bending energy of the sheet, which has Young's modulus E and Poisson ratio ν so that the bending stiffness $B = Eh^3/12(1-\upsilon^2)$. The second term represents the adhesive penalty per unit length due to delamination. The third term corresponds to the constraint of inextensibility, which is enforced by the Lagrange multiplier α.

In the second term of eqn (1), $\Delta\gamma = \gamma_{sv}^{(sheet)} + \gamma_{sv}^{(substrate)} - \gamma_{ss}$, where γ_{sv} represents the solid–vapour surface energy and γ_{ss} the solid–solid energy for the sheet–substrate interface.† Generally, delamination is composed of fracture in a combination of modes I and II. The interfacial energy $\Delta\gamma$ is therefore a function of the relative amounts of each mode present in a given scenario. However, for blisters much larger than the thickness of the sheet, this fraction is independent of shape and so $\Delta\gamma$ may be assumed constant.[25]

Using the Calculus of Variations allows us to determine equations for the shape of the delaminated blister, $\theta(s)$, and the length of the delaminated portion, l_b, which extremize the functional U given in eqn (1). The requirement that $\delta U/\delta\theta = 0$ yields the classical Elastica equation for a free sheet that experiences a constant compressive stress T:[26,27]

$$B\theta_{ss} = -T\sin\theta, \quad (2)$$

where the Lagrange multiplier $\alpha \to -T$. The requirement that $\delta U/\delta l = 0$ yields a condition on the curvature at contact†,[8,22,28,29]

$$\theta_s(\pm l_b/2) = \sqrt{2}/\ell_{ec}, \quad (3)$$

where $\ell_{ec} = (B/\Delta\gamma)^{1/2}$ is the *elasto-capillary* length of the system.[30] We note that eqn (2) is the classic Elastica equation and hence that the shape of the delamination blister is precisely that of an Elastica with the same arc length l_b and compression Δl. The crucial difference between the classic Elastica and the 'Sticky Elastica' is the following: the former has a fixed arc length while the arc length of the latter changes in response to compression to ensure that the curvature at the end point satisfies eqn (3).

It is well known that it is possible to make some analytical progress for the nonlinear eqn (2), which also describes the motion of a constant length pendulum (with arc length replaced by time). However, it is instructive to consider first the linearized problem, *i.e.* the small deformation limit. In this limit, $\theta(s) \ll 1$ and geometrical considerations give us that $\theta \sim d/\ell$, where d is the blister height and ℓ its width. Since eqn (3) gives us that $\theta_s \sim 1/\ell_{ec}$ and $\ell \approx l_b$ (for small deformations) we then have that $d/\ell^2 \sim 1/\ell_{ec}$. A more careful analysis shows[3] that, in fact,

$$d/\ell^2 \approx \frac{1}{2^{1/2}\pi^2}\ell_{ec}^{-1}. \quad (4)$$

Referring to the quantity d/ℓ^2 as the typical curvature of the blister we see that, for small deformations at least, the typical curvature is a constant multiple of ℓ_{ec}^{-1}, independently of the dimensions of the blister.[3,4] This result is therefore a simple, yet useful method for measuring the elastocapillary length of a system. The question arises, however, of how this result is modified for blisters beyond the small deformation limit? On dimensional grounds d/ℓ^2 must still scale like ℓ_{ec}^{-1} but, as we shall see, the (dimensionless) aspect ratio d/ℓ also plays a role.

To facilitate our analysis, we first non-dimensionalize the system by letting $\tau = T/\Delta\gamma$, $\delta = d/\ell_{ec}$, $\lambda = \ell/\ell_{ec}$, $S = s/\ell_{ec}$, $L = l_b/\ell_{ec}$, *etc.* The Elastica eqn (2) then becomes $\theta_{ss} = -\tau\sin\theta$, with boundary condition $\theta_s(\pm L/2) = \sqrt{2}$. Integrating once and imposing the latter condition, we find that the compressive stress τ and maximum angle θ_0 are related by $\tau = 1/(1-\cos\theta_0)$, giving

$$\theta_S^{\,2} = 2\,\frac{\cos\theta - \cos\theta_0}{1-\cos\theta_0}, \quad (5)$$

where θ_0 is defined as the angle at which the curvature vanishes, *i.e.* the maximum value of θ within the sheet. By symmetry, we have that $\theta(-L/2) = \theta(0) = \theta(L/2) = 0$. The angle θ must therefore

increase from 0 at $S = -L/2$ up to θ_0 and subsequently decrease from θ_0 to match $\theta = 0$ at $S = 0$. The symmetry of the problem therefore dictates that an inflection point $\theta_S = 0$ must occur at $S = \pm L/4$ so that

$$\theta_S = \sqrt{2}\left(\frac{\cos\theta - \cos\theta_0}{1-\cos\theta_0}\right)^{1/2} \times \begin{cases} -1, 0 \leqslant |S| < L/4, \\ +1, L/4 \leqslant |S| \leqslant L/2. \end{cases} \quad (6)$$

We note that this requires that the blister is not only symmetric around $S = 0$ but, further, that the segment $L/4 < |S| < L/2$ is a rotation by 180° of the segment $0 < |S| < L/4$. This rotational and reflectional symmetry (illustrated in Fig. 1) is easily appreciated when considering the analogy between the motion of a pendulum and the shape of an elastica.[19] Within this analogy, the four segments of the elastica correspond to the four phases of the pendulum, which are clearly symmetric around the pendulum's lowest point and time reversed around its highest point.

To make further progress requires the determination of the unknown angle θ_0, which in turn requires a relationship between the compression applied, ΔL, and θ_0. Using the symmetry of the problem just discussed, we have that

$$\Delta L = 4\int_0^{L/4} (1-\cos\theta)\mathrm{d}S.$$

Making use of the substitution $\mathrm{d}S = \mathrm{d}\theta/\theta_S$ and integrating from $\theta = 0$ to $\theta = \theta_0$, we find that:

$$\Delta L = 2^{5/2}(1-\cos\theta_0)(F[\boldsymbol{q}] - E[\boldsymbol{q}]), \quad (7)$$

where $\boldsymbol{q} = (\theta_0/2, \csc^2\theta_0/2)$, and $F[\ldots]$ and $E[\ldots]$ are the elliptical integrals of the first and second kind, respectively.[31] The expression (7) in principle allows us to obtain the maximum angle as a function of end-to-end compression, $\theta_0 = \theta_0(\Delta L)$, numerically. Once θ_0 is determined, it is a simple matter to calculate the dimensions of the blister as

$$\begin{aligned} \delta &= \int_{-L/2}^{0} \sin\theta \mathrm{d}S = 2^{3/2}(1-\cos\theta_0), \\ \lambda &= \int_{-L/2}^{L/2} \cos\theta \mathrm{d}S = 2^{5/2}\{(1-\cos\theta_0)E[q] + \cos\theta_0 F[q]\}. \end{aligned} \quad (8)$$

Plots of the (numerically determined) evolution of the blister dimensions with increasing compression are given for $\lambda = \lambda(\Delta L)$ in Fig. 3a and for $\delta = \delta(\Delta L)$ in Fig. 3b.

The shape of the blister $[X(S), W(S)]$ can also be determined using analogous integrals, and compared with experimental results (see Fig. 2). We also find that at a critical compression, $\Delta L^* \approx 8.71949$ (corresponding to $\lambda^* \approx 1.55502$, $\delta^* \approx 4.13610$) the sheet comes into self-contact, forming a perfect "S" shape.

3 Asymptotic results

While the solution in terms of elliptic integrals is relatively simple to implement computationally, it is of limited use in experimental settings. We therefore consider some asymptotic results for $\Delta L \ll 1$. We shall see that these give a very good account of the numerical results, even up to self-contact.

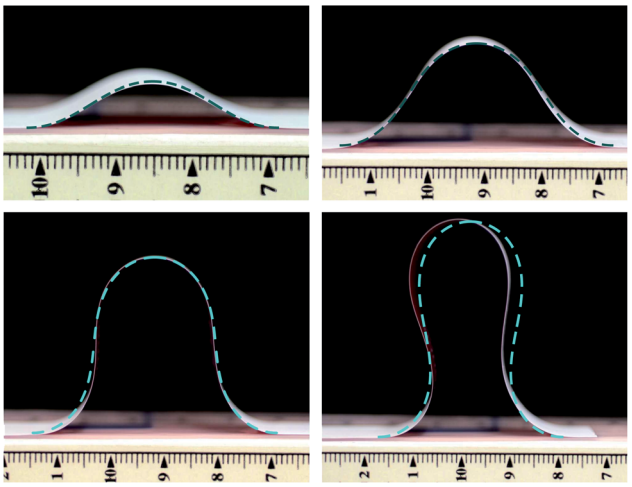

Fig. 2 The '*Sticky Elastica*' for $\Delta L = 0.18, 1.12, 3.25, 5.63$, ($\ell_{ec} = 1.35$ cm). In each case the theoretical prediction obtained using the experimentally measured value of Δl gives a good account of the experimentally observed blister shape (dashed curves). Here the sheet thickness $h = 70$ μm, corresponding to black triangles in Fig. 3 and 4. Note that there is a loss of symmetry for the largest compression. We believe this to be an effect of the small, but finite, weight of the sheet since the 'heavy' elastica is subject to just such an instability.[24,32]

The asymptotic result in eqn (4) may be found by considering the leading order behaviour. However, it is possible to do better by retaining higher order terms in the θ_0 power series expansions of δ, λ and ΔL. By eliminating θ_0 in favour of ΔL we find that†

$$\lambda = 2\pi^{2/3}\Delta L^{1/3} - \frac{7}{8}\Delta L + \ldots, \quad (9)$$

$$\delta = 2\sqrt{2}\left(\frac{\Delta L}{\pi}\right)^{2/3} - \frac{1}{2\sqrt{2}}\left(\frac{\Delta L}{\pi}\right)^{4/3} + \ldots. \quad (10)$$

The one-term and two-term asymptotic expansions for $\lambda(\Delta L)$ and $\delta(\Delta L)$ are shown in Fig. 3a and b, respectively. These demonstrate that, although only strictly being valid for $\Delta L \ll 1$, the two-term expansion compares extremely well with the numerical results even for $\Delta L \approx 8$, *i.e.* close to self-contact. We also note that the evolution of $\lambda(\Delta L)$ is non-monotonic (see Fig. 3a), decreasing for $\Delta L \gtrsim 64\pi/21^{3/2} \approx 2.0894$. While the asymptotic expression for δ likewise predicts a maximum height, this only occurs for $\Delta L \approx 8\pi$, which is far beyond the point of self-contact, ΔL^* (and hence is not physically realizable).

The non-monotonicity of the blister width, λ, has been observed in other, related, systems[33] but is not observed with the classic Elastica, for which λ decreases monotonically as the compression is increased. The non-monotonic behaviour observed for the Sticky Elastica is caused by the fact that the arc length of the blistered region initially increases rapidly with increasing compression; this increasing length of the buckled

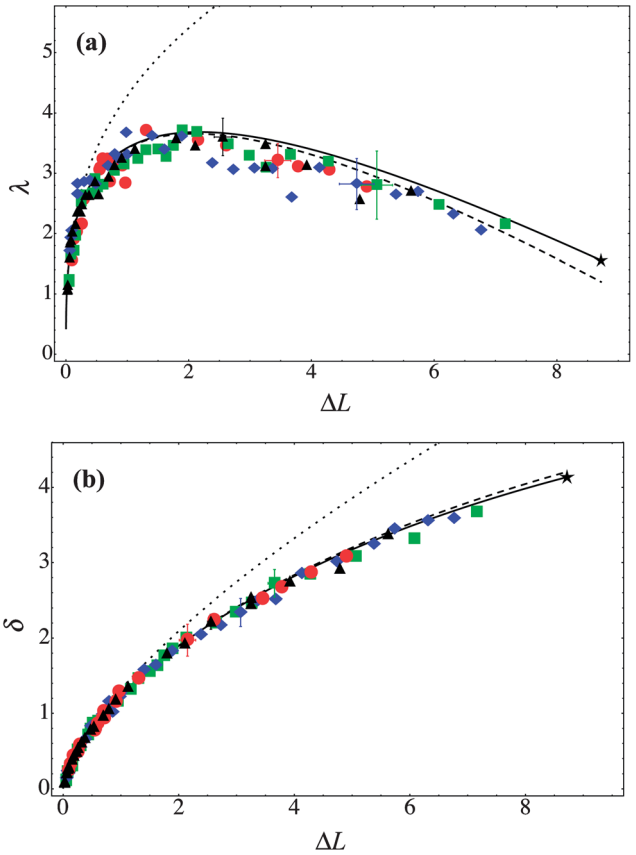

Fig. 3 (a) Blister width, λ, as a function of the compression ΔL. The full numerical solution (solid black curve) is partially captured by the first term of the asymptotic expression (dotted). The two term asymptotic approximation (eqn (9)) (dashed) gives a much better prediction and explains the non-monotonic behaviour. Points refer to experimental results obtained with different sheets. Sheet thicknesses are: $h_1 = 52$ μm (●), $h_2 = 42$ μm (■), $h_3 = 41$ μm (◆) and $h_4 = 70$ μm (▲). Self-contact occurs at $\Delta L^* \approx 8.719$, $\lambda^* \approx 1.555$ (★). (b) Blister height, $\delta(\Delta L)$, with asymptotic approximations given by eqn (10). The height at self-contact is $\delta^* \approx 4.136$. All lengths are non-dimensionalized by ℓ_{ec}, determined using the method described later. Typical error bars are shown for each series of experiments.

region overcomes the decrease caused by compression and so λ initially increases with ΔL. However, with still larger compression, the increase of arc length slows and is not large enough to keep up with the imposed compression: λ reaches a maximum value and begins to decrease. It is also interesting to observe that, except for very small compressions ($\Delta L \lesssim 0.3$), the dependence of blister width on ΔL is relatively weak; we therefore propose that, as a rule of thumb, $\lambda \approx 3\ell_{ec}$. This result provides a quick way to get a rough estimate for the elasto-capillary length by looking just at the typical width of the blisters in a system. This gives further justification to the assumption that the blister width is roughly constant in delamination buckling, an assumption often called upon in previous work.[25]

Using the asymptotic results from eqn (9) and (10), we can return to the question of central interest here: how does the typical curvature d/ℓ^2 relate to the elastocapillary length? We find that the typical curvature can be expressed simply by eliminating ΔL in favour of δ/λ, the aspect ratio of the blister:

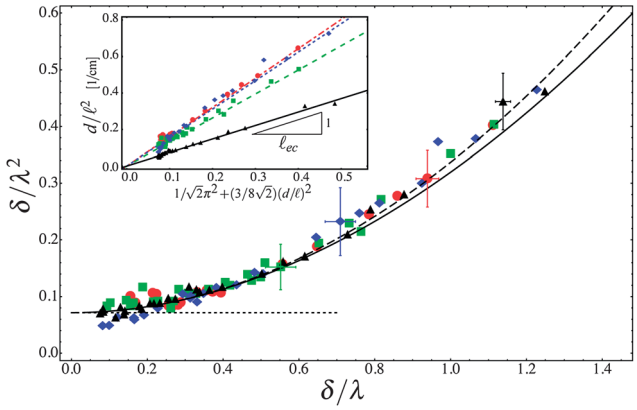

Fig. 4 Dimensionless typical curvature of blisters δ/λ^2 as a function of the aspect ratio δ/λ. Shown are the full numerical solution (solid black), along with the first order (dotted) and second order asymptotic approximations (eqn (11)), (dashed). Points refer to different thickness sheets: $h_1 = 52$ μm (●), $h_2 = 42$ μm (■), $h_3 = 41$ μm (◆) and $h_4 = 70$ μm (▲). The point of self-contact lies outside the plot range shown, at $\delta^*/\lambda^* \approx 2.660$, $\delta^*/\lambda^{*2} \approx 1.710$. All lengths are non-dimensionalized by ℓ_{ec}. Error bars are representative of each set of experiments. Inset: Determination of the elasto-capillary length, ℓ_{ec}, from the dimensional value of the typical curvature d/ℓ^2, for the four sets of experiments discussed. The straight lines represent best fits to the raw data whose slope provides an estimate for the quantity $1/\ell_{ec}$.

$$\frac{\delta}{\lambda^2} = \frac{1}{\sqrt{2}\pi^2} + \frac{3}{8\sqrt{2}}\left(\frac{\delta}{\lambda}\right)^2 - \ldots. \qquad (11)$$

Thus, in the limit of small blisters we recover the result (4). However, as δ/λ increases the typical curvature grows roughly quadratically. The asymptotic relationship (11) agrees with the results of numerical calculations, as shown in Fig. 4.

4 Experiments

The preceding theoretical analysis was tested using a set of desktop experiments at a macroscopic scale. We used plastic sheets of different thicknesses adhered to tacky rubber surfaces (fabricated from Zhermack dental polymer). The sheets used were uniform strips of adhesive tape (thickness $h_1 = 52$ μm, red circles in Fig. 3 and 4) and other thin elastic sheets without an adhesive coating, which were obtained from the labels of commonly available drink bottles (Aquafina, $h_2 = 42$ μm, green squares; Copella, $h_3 = 41$ μm, blue diamonds; and Vitamin Water $h_4 = 70$ μm, black triangles in Fig. 3 and 4). The Young's modulus of these sheets was measured to be $E = 0.7 \pm 0.1$ GPa using the deflection of the sheets under their own weight.

For the adhesion experiments described here, the sheets were cut into strips of width 1 cm and length 10 cm. The ends of these strips were brought together by a distance Δl and the strip then brought into contact with the substrate. Upon deposition the strip was forced into adhesion beyond its equilibrium state by applying pressure over almost the entire strip (missing out the central blistered part and avoiding the plastic deformations that occur for very high curvatures). Once the external pressure is removed, the strip spontaneously deadheres until reaching an equilibrium state in which the length of its deadhered portion, l_b, is well-defined, as shown in Fig. 2. The results of

experiments performed in this way were robust and reproducible.

The dimensions d and ℓ of the blisters in equilibrium were measured for a range of the end–end compression Δl. A comparison of experimental and theoretical predictions is given in Fig. 3 and 4. To plot these in the dimensionless form the elastocapillary length for each strip–substrate pair had to be determined. This was done by plotting the dimensional values of d/ℓ^2 against the dimensionless quantity $1/\sqrt{2}\pi^2 + (3/8\sqrt{2})(d/\ell)^2$ — eqn (11) leads us to expect that such a plot should yield a straight line with a slope $1/\ell_{ec}$ allowing the value of ℓ_{ec} to be estimated. Such a plot is shown in Fig. 4 (inset) and demonstrates the expected linear behaviour. We therefore believe that this method represents an effective method for determining the elastocapillary length in scenarios where the aspect ratio d/ℓ is not small. We find for the adhesive tape $\ell_{ec}^{(1)} = 0.62$ cm and for the non-adhesive tapes $\ell_{ec}^{(2)} = 0.76$ cm, $\ell_{ec}^{(3)} = 0.64$ cm and $\ell_{ec}^{(4)} = 1.35$ cm. From this we infer for the adhesive tape $\Delta\gamma^{(1)} \simeq 0.25$ J m^{-2} and for the non-adhesive tapes $\Delta\gamma^{(2-4)} \simeq 0.08$–$0.13$ J m^{-2}. This is comparable to values obtained in similar studies.[3]

The agreement between theory and experiment shown in Fig. 3 and 4 seems to be reasonably robust given the relative difficulty in measuring the exact blister width ℓ (rather than blister height d, which is much easier to measure). This is particularly important in Fig. 4, due to the ℓ^{-2} dependence of the typical curvature and the $(d/\ell)^2$ term in eqn (11). We note from both figures that the agreement between experimental and asymptotic results is better than that between experimental and numerical results; we attribute this to the fact that the value of ℓ_{ec} was determined by using the asymptotic result (11), rather than the full theoretical solution. Attempts to use higher order asymptotic expansions fail because of the compounding of the error in the measurement of ℓ that occurs when computing $(d/\ell)^4$ and higher order terms.

5 Conclusions

In this article we have presented numerical results for the shape and dimensions of delamination blisters allowing for the possibility that the slope of the blister may not be small. An asymptotic analysis yielded simple expressions for the dimensions of the blisters, which are in excellent agreement with numerical results up to the point of self-contact, where $\Delta L \approx 8$. This is particularly striking, since the asymptotic calculations are only strictly valid in the limit $\Delta L \ll 1$. The success of these asymptotic results also enabled us to propose a straightforward way to estimate the strength of adhesion based on the geometry of delamination blisters beyond the limit of small deformations. We tested this technique with a series of simple table-top experiments obtaining good agreement between experiment and theory with a single fitting parameter: the elastocapillary length ℓ_{ec}, which relates the bending rigidity of the film and the adhesive energy.

Our study was motivated by the controlled use of delamination in technologies at small scales, most notably in flexible electronics. In these situations, the deformation of the delaminated components is often not small and so we expect that our results would be of use in such applications, albeit provided that a simple adhesion is used, rather than the patterning that is currently common.[13] In our analysis, we have assumed that there is no relative motion between the strip and the substrate. In reality, this can be achieved in two ways: (i) the sheet is confined *before* it is brought in contact with the rigid substrate (as in the experiments presented here) or (ii) the (relatively stiff) strip is initially flat and adhered to a compressible substrate. If the *entire* strip–substrate system is then compressed, the strip is forced to buckle out of plane and delaminate from the substrate forming a delamination blister. For our analysis to be applicable to this latter case, we require that the surface energy decrease due to the decrease in the substrate surface during compression is small, *i.e.* that $\gamma_{sv} \ll \gamma_{ss}$.†

The main difference to canonical studies of delamination is that the width of the blister is not fixed *a priori* but is rather determined by a balance between bending and adhesive forces at a fixed compression Δl. Nevertheless, our analysis shows that, in fact, as the compression is increased the preferred size of this blister changes only very slightly.

An important feature of blisters in flexible electronic applications is that the buckled components should retain a sufficiently small curvature that they do not deform plastically under repeated flexing. Here, we assume that this condition is satisfied provided that the stress within the beam, σ, does not reach the yield stress, σ_y. From linear elasticity theory, the maximum bending stress within a sheet occurs at the surfaces $z = \pm h/2$ of the sheet. Therefore, if the sheet is deformed to have a maximum curvature $|\theta_s|_{Max}$ then $\sigma_{Max} = Eh|\theta_s|_{Max}/2(1 - \upsilon^2)$[34] and we have that no failure will occur provided that

$$\sigma_y > \sigma_{Max} = \frac{Eh}{2(1-\nu^2)}|\theta_s|_{Max}. \quad (12)$$

However, our analysis has shown that for the Sticky Elastica, the maximum curvature occurs at $s = 0, \pm l/2$ and has value $|\theta_s|_{Max} = \sqrt{2}/\ell_{ec}$, see eqn (3). Buckling will therefore occur without plastic deformation provided that

$$\frac{{\sigma_y}^2 h}{E\Delta\gamma} > \frac{6}{1-\nu^2}, \quad (13)$$

i.e. provided that the thickness is large enough for given material properties, or provided the substrate–strip adhesion is sufficiently weak. We note that this result is precisely the same as that derived previously from linear considerations[3] but applies independently of the degree of compression, since the maximum curvature is given solely by the elastocapillary length ℓ_{ec}. In other words, the sheet is no more likely to fail for larger compressions than for the initial delamination event – if it survives the original deformation it can safely be compressed further.

This publication is based on work supported in part by Award no. KUK-C1-013-04, made by King Abdullah University of Science and Technology (KAUST). TJWW is supported by EPSRC.

References

1 G. Gioia and M. Ortiz, *Adv. Appl. Mech.*, 1997, **33**, 119–192.
2 S. Faulhaber, C. Mercer, M. W. Moon, J. W. Hutchinson and A. G. Evans, *J. Mech. Phys. Solids*, 2006, **54**, 1004–1028.
3 D. Vella, J. Bico, A. Boudaoud, B. Roman and P. M. Reis, *Proc. Natl. Acad. Sci. U. S. A.*, 2009, **106**, 10901–10906.
4 Y. Aoyanagi, J. Hure, J. Bico and B. Roman, *Soft Matter*, 2010, **6**, 5720–5728.
5 E.-A. Kim and A. H. Castro Neto, *EPL*, 2008, **84**, 57007.
6 H. C. Schniepp, K. N. Kudin, J. L. Li, R. K. Prudhomme, R. Car, D. A. Saville and I. A. Aksay, *ACS Nano*, 2008, **2**, 2577–2584.
7 Z. Li, Z. Cheng, R. Wang, Q. Li and Y. Fang, *Nano Lett.*, 2009, **9**, 3599–3602.
8 J. W. Obreimoff, *Proc. R. Soc. London, Ser. A*, 1930, **127**, 290–297.
9 H. M. Jensen, *Eng. Fract. Mech.*, 1991, **40**, 475–486.
10 K. T. Wan, *J. Adhes.*, 1999, **70**, 209–219.
11 J. Chopin, D. Vella and A. Boudaoud, *Proc. R. Soc. A*, 2008, **464**, 2887–2906.
12 S. P. Koenig, N. G. Boddeti, M. L. Dunn and J. S. Bunch, *Nat. Nanotechnol.*, 2011, **6**, 543–546.
13 Y. Sun, W. M. Choi, H. Jiang, Y. Y. Huang and J. A. Rogers, *Nat. Nanotechnol.*, 2006, **1**, 201–207.
14 D. Y. Khang, J. A. Rogers and H. H. Lee, *Adv. Funct. Mater.*, 2009, **19**, 1526–1536.
15 J. A. Rogers, T. Someya and Y. Huang, *Science*, 2010, **327**, 1603–1607.
16 H. Cheng, J. Wu, M. Li, D. H. Kim, Y. S. Kim, Y. Huang, Z. Kang, K. C. Hwang and J. A. Rogers, *Appl. Phys. Lett.*, 2011, **98**, 061902.
17 Y. Ebata, A. B. Croll and A. J. Crosby, *Soft Matter*, 2012, 9086–9091.
18 Z. Chen, B. Cotterell and W. Wang, *Eng. Fract. Mech.*, 2002, **69**, 597–603.
19 R. Levien, *The Elastica: a Mathematical History*, EECS Department, University of California, Berkeley technical report, 2008.
20 R. H. Plaut, S. Suherman, D. A. Dillard, B. E. Williams and L. T. Watson, *Int. J. Solids Struct.*, 1999, **36**, 1209–1229.
21 A. A. Colom, *Am. J. Phys.*, 2006, **74**, 633.
22 N. J. Glassmaker and C. Y. Hui, *J. Appl. Phys.*, 2004, **96**, 3429.
23 A. E. Cohen and L. Mahadevan, *Proc. Natl. Acad. Sci. U. S. A.*, 2003, **100**, 12141.
24 D. Vella, A. Boudaoud and M. Adda-Bedia, *Phys. Rev. Lett.*, 2009, **103**, 174301.
25 J. W. Hutchinson and Z. Suo, *Adv. Appl. Mech.*, 1992, **29**, 191.
26 A. E. H. Love, *A Treatise on the Mathematical Theory of Elasticity*, Dover, New York, 1944.
27 B. Audoly and Y. Pomeau, *Elasticity and Geometry*, Oxford University Press, 2010.
28 L. D. Landau and E. M. Lifschitz, *The Theory of Elasticity*, Pergamon, 1970.
29 C. Majidi, *Mech. Res. Commun.*, 2007, **34**, 85–90.
30 J. Bico, B. Roman, L. Moulin and A. Boudaoud, *Nature*, 2004, **432**, 690.
31 F. W. Olver, D. W. Lozier, R. F. Boisvert and C. W. Clark, *NIST Handbook of Mathematical Functions*, Cambridge University Press, 1st edn, 2010.
32 G. Domokos, W. B. Fraser and I. Szeberényi, *Phys. D (Amsterdam, Neth.)*, 2003, **185**, 67–77.
33 T. J. W. Wagner and D. Vella, *Phys. Rev. Lett.*, 2011, **107**, 044301.
34 E. H. Mansfield, *The Bending and Stretching of Plates*, Cambridge University Press, 1989.

